

# Electronic and ionic conduction in some simple lithium salts

H. B. LAL, KANCHAN GAUR, A. J. PATHAK

*Department of Physics, University of Gorakhpur, Gorakhpur 273 009, India*

The electrical conductivity ( $\sigma$ ) and thermoelectric power ( $S$ ) of solidified melt samples of  $\text{Li}_2\text{MoO}_4$ ,  $\text{Li}_2\text{WO}_4$  and  $\text{Li}_2\text{SO}_4$  are presented in the temperature range 415 K to melting point of each compound. The ratio of ionic to electronic contribution to  $\sigma$  has been obtained with the help of a time-dependence study of d.c. electrical conductivity. It has been shown that in  $\text{Li}_2\text{MoO}_4$  electronic contribution to  $\sigma$  remains high up to its melting point (about 8% just below the melting point) and it shows no superionic phase. However, in  $\text{Li}_2\text{WO}_4$  and  $\text{Li}_2\text{SO}_4$  a superionic phase is obtained in which the ionic contribution to  $\sigma$  is more than 99.99%. However, in normal ionic (or  $\alpha$ ) phase it is small and decreases with decreasing temperature. Separate temperature variations of ionic ( $\sigma_i$ ) and electronic ( $\sigma_e$ ) conductivities are presented and the conduction mechanisms are discussed. It is shown that ionic conduction in the  $\beta$ -phase is dominated by Schottky-type defects.

## 1. Introduction

The electrical conductivity of simple lithium salts has been studied by many workers [1-6] in order to search lithium-ion conducting superionic solids. However, no attempt has been made so far to estimate relative contributions of ionic and electronic conductivities in them, which is essential to judge their potential for application in electrochemical devices. Further, most of the studies on these compounds are confined either to the superionic phase just below their melting point [2, 3] or to the low-conducting  $\beta$ -phase [4-8]. No systematic approach has been made to study them over a wide temperature range (from room temperature to their melting point). This lack of study prompted us to re-examine these salts from the above points of view. This paper is an attempt in this direction and presents the study of  $\text{Li}_2\text{MoO}_4$ ,  $\text{Li}_2\text{WO}_4$  and  $\text{Li}_2\text{SO}_4$  solidified melt. The electrical transport, in general, has also been examined and some new results, not reported so far, have been obtained and discussed.

## 2. Material preparation and experimental technique

$\text{Li}_2\text{SO}_4$  with stated purity of 99.99% was procured from Rare and Research Chemicals, Bombay, India;  $\text{Li}_2\text{MoO}_4$  and  $\text{Li}_2\text{WO}_4$  were prepared in the laboratory. The starting materials for the preparation of these compounds were  $\text{Li}_2\text{O} + \text{MoO}_3$  and  $\text{Li}_2\text{O} + \text{WO}_3$ , respectively, all with stated purity of 99.99% (Rare and Research Chemicals, Bombay, India). Starting materials were taken in the ratio of their molecular weight and were thoroughly mixed and fired in air in a silica crucible for 48 h with one intermediate grinding. The firing temperature in case of  $\text{Li}_2\text{MoO}_4$  was 740 K and for  $\text{Li}_2\text{WO}_4$  it was 800 K. The measurement of electrical conductivity was done on a solidified melt. A self-designed sample holder has been

used for this purpose. It consists of a Corning flat-bottom test tube in which two flat silver electrodes of equal size and area are fixed parallel to each other. These two electrodes are joined by two thick silver wires for external connections. The material whose conductivity is to be measured is poured into sample holder and pressed. It is then heated until the salt inside it melts. It is slowly cooled to room temperature. The outer electrodes are then connected to the measuring instrument. The measurement of  $\sigma$  was done using the sample holder and procedure described elsewhere [9, 10].

## 3. Results and discussion

The electrical conductivity,  $\sigma$ , and thermoelectric powers,  $S$ , of  $\text{Li}_2\text{MoO}_4$ ,  $\text{Li}_2\text{WO}_4$  and  $\text{Li}_2\text{SO}_4$  prepared in different lots have been measured as a function of temperature. Measurements were done in both heating and cooling cycles. No appreciable difference was noticed in the values of  $\sigma$  and  $S$  in the heating and cooling cycles. The results are shown in Figs 1 to 3 as  $\log \sigma T$  against  $T^{-1}$  and  $S$  against  $T^{-1}$  plots. The electrical conductivity of the salts studied has been measured by different workers in the past. A comparison of these data is given in Table I. It is seen from this table that there exists fair agreement between the  $\sigma$  data reported by different workers. The minor difference existing is perhaps due to different forms of the sample and electrodes used by the different workers.

The contribution to electrical conductivity is due to migration of ions or electrons, or both. The theories for ionic and electronic conduction are significantly different. Hence to present any meaningful discussion of electrical conduction, one has to distinguish whether the conductivity is predominantly electronic or ionic. There are conventional methods to do this [11, 12], but a much easier method is to measure  $\sigma_{\text{d.c.}}$  as a function

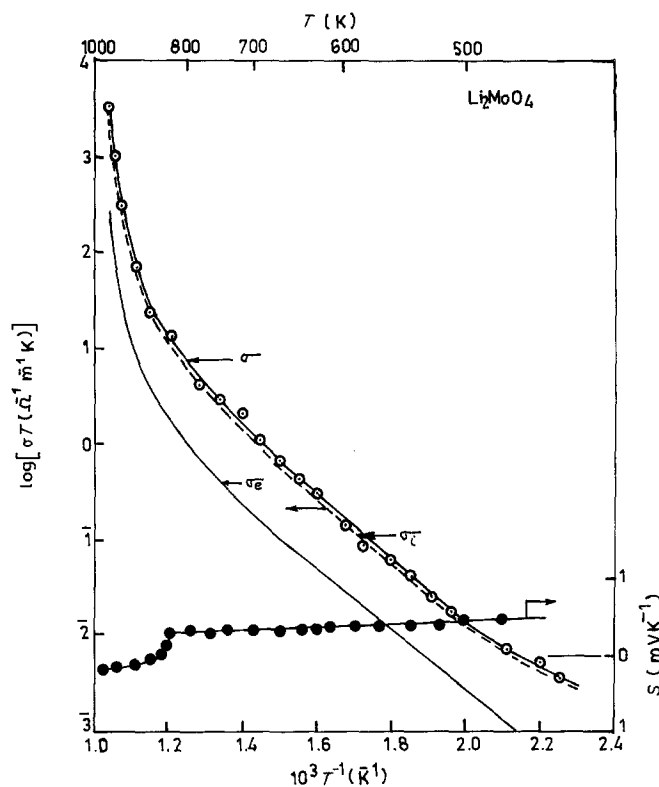


Figure 1 Plots of  $\log \sigma T$ ,  $\log \sigma_i T$ ,  $\log \sigma_e T$  and  $S$  against  $1/T$  for lithium molybdate.

of time with an electrode that blocks ionic conduction but not the electronic conduction. A time-dependent d.c. electrical conductivity normally occurs in solids with ionic conduction, if the electrodes used for this measurement are capable of blocking the flow of ions. When an electric field is applied through a potential on the two electrodes, positive ions move in the direction of the applied field and negative ions opposite to it. Because electrodes are blocking the path of ions, they are not able to discharge at the electrodes and begin to accommodate at the electrodes. This creates a field opposite to that of the applied field. Thus the net force acting on the ions trying to move towards the electrode decreases and fewer ions are able to reach electrode and the d.c. current decreases. With time the opposing field grows and tends to become equal to the applied field after a long time ( $t \rightarrow \infty$ ). Thus in pure

ionic solids, the d.c. current decreases and tends to become zero after a very long time.

Extending the above argument to the case of a mixed ionic conductor, one expects a continuous decrease in current which should tend to acquire constant value after a long time. This current arise because the electric field does not become zero due to polarization produced by the ions. The transient appears due to ionic charges; hence once these transients have died out, the remaining constant value of current can be totally assigned to electrons [13–15]. The initial current (current at  $t = 0$ ) is the total current contributed by both ions and electrons. Thus from time-dependent measurement of the current we can evaluate the total as well as the ionic and electronic parts of the conductivity.

We have performed a time-dependence study of  $\sigma$  at

TABLE I Relevant data of electrical conductivity reported by different workers

Compound	Form <sup>†</sup>	$\sigma^*$ ( $\Omega^{-1} \text{ m}^{-1}$ )	$T$ (K)	$E_a$ (eV)	Phase	Reference
$\text{Li}_2\text{MoO}_4$	P	10	970	—	—	[16]
	P	$2.5 \times 10^{-4}$	500	0.73 <sup>‡</sup>	—	[16]
	SM	12	970	—	—	Present work
	SM	$3.2 \times 10^{-4}$	500	0.67 <sup>‡</sup>	—	Present work
$\text{Li}_2\text{WO}_4$	SM	143	973	0.36	$\alpha$	[3]
	P	18	973	0.25 <sup>‡</sup>	$\alpha$	[17]
	P	$3.2 \times 10^{-14}$	500	0.75 <sup>‡</sup>	$\beta$	[17]
	SM	145	973	0.25 <sup>‡</sup>	$\alpha$	Present work
$\text{Li}_2\text{SO}_4$	SM	$1.26 \times 10^{-3}$	500	0.85 <sup>‡</sup>	$\beta$	Present work
	SM	300	1073	—	$\alpha$	[1]
	SM	200	1000	0.36	$\alpha$	[2]
	SM	200	1000	0.43 <sup>‡</sup>	$\alpha$	[18]
	SM	171	1000	0.41 <sup>‡</sup>	$\alpha$	Present work
	P	$3.2 \times 10^{-5}$	700	0.74	$\beta$	[7]
	P	$5.0 \times 10^{-4}$	700	1.2	$\beta$	[8]
	SM	$2.64 \times 10^{-3}$	700	1.12 <sup>‡</sup>	$\beta$	Present work

\*Obtained from graphical plots.

<sup>†</sup>P, pressed pellet; SM solidified melt.

<sup>‡</sup>Slope of  $\log \sigma T - T^{-1}$  plot.

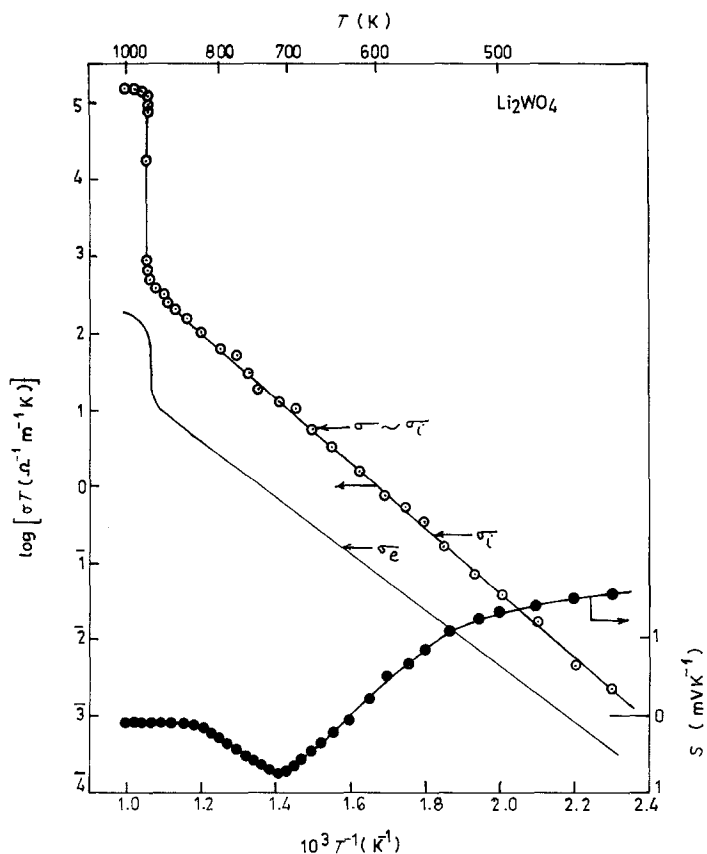


Figure 2 Plots of  $\log \sigma T$ ,  $\log \sigma_i T$ ,  $\log \sigma_e T$  and  $S$  against  $1/T$  for lithium tungstate.

low but constant electric field and temperature. Typical plots are shown in Fig. 4. The plots at other temperatures have a similar nature. It is observed from this figure that, in general,  $\sigma$  decreases with time and tends to become constant. The trend of constancy begins to appear after a short interval of time at lower temperature, but increases with increasing temperature. The constant value of  $\sigma_{d.c.}$  after a long time ( $t \rightarrow \infty$ ) is the electronic part ( $\sigma_e$ ) of the conductivity and the value of  $\sigma_{d.c.}$  for  $t \rightarrow 0$  is the total (ionic + electronic) conductivity.

In order to check whether  $\sigma_{d.c.}(0)$  corresponds to true conductivity,  $\sigma$  was measured at a few fixed frequencies. The results are shown in Fig. 5. It is seen from this figure that there exists no difference between  $\sigma_{d.c.}(0)$  and  $\sigma_{a.c.}$  values. This indicates that grain-boundary effects are not important and no pores exist in the samples. This is an expected result, as solidified melt samples have a density very close to their X-ray densities, as shown in Table II. A time-dependence study of  $\sigma_{d.c.}$  has been performed at six or seven widely separated temperatures and at each temperature

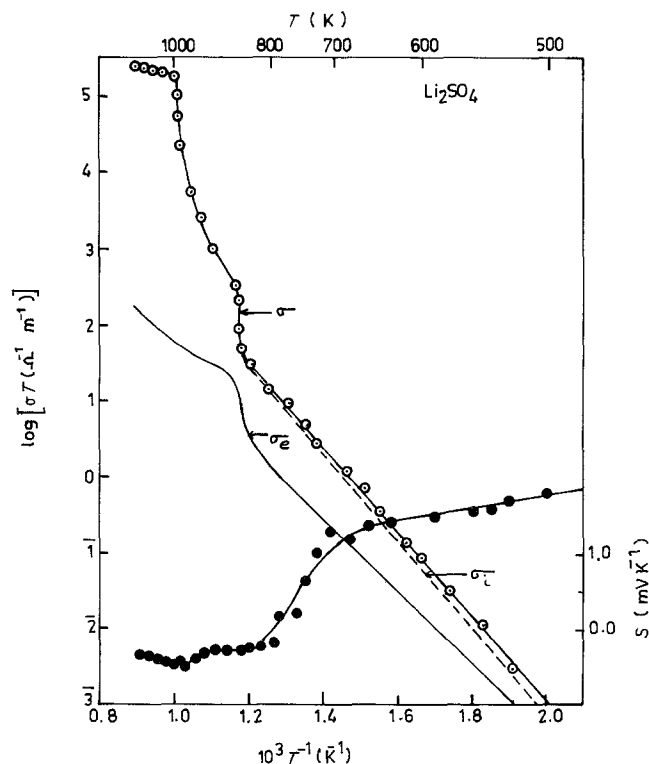


Figure 3 Plots of  $\log \sigma T$ ,  $\log \sigma_i T$ ,  $\log \sigma_e T$  and  $S$  against  $1/T$  for lithium sulphate.

TABLE II Structural parameters at room temperature, melting point ( $T_m$ ) and X-ray and measured densities of the studied compounds

Compound	Unit cell*	Unit cell parameters (nm)			$\alpha/\beta$ (deg)	Reference	$T_m$ (K)	Density ( $\text{kg m}^{-3}$ ) $10^{-3}$	
		$a$	$b$	$c$				X-ray	Measured
$\text{Li}_2\text{MoO}_4$	R	0.877	–	–	108.17	[19]	978	2.70	2.66
$\text{Li}_2\text{WO}_4$	R	0.877	–	–	108.17	[19]	1015	4.07	4.02
$\text{Li}_2\text{SO}_4$	M	0.824	0.495	0.847	107.99	[20]	1133	2.22	2.18

\*R, rhombohedral; M, monoclinic.

$\sigma_{\text{d.c.}}(0)$  and  $\sigma_{\text{d.c.}}(\infty)$  have been obtained. Using these values, the ratio of ionic to electronic conductivities ( $r = \sigma_i/\sigma_e$ ) has been obtained using the relation

$$\begin{aligned} \gamma &= \frac{\sigma_i}{\sigma_e} \\ &= \frac{\sigma - \sigma_e}{\sigma_e} \\ &= \frac{\sigma_{\text{d.c.}}(0) - \sigma_{\text{d.c.}}(\infty)}{\sigma_{\text{d.c.}}(\infty)} \end{aligned} \quad (1)$$

A plot of  $\log r$  against temperature is shown in Fig. 6. From this figure one can estimate the contribution of ionic and electronic conductivity to the total conductivity at any temperature using the relation

$$\sigma_i = \left( \frac{r}{r+1} \right) \sigma \quad (2)$$

$$\sigma_e = \left( \frac{1}{r+1} \right) \sigma \quad (3)$$

To show this more clearly, the percentage of ionic and electronic contribution to  $\sigma$  in the solids studied at different temperatures is given in Table III. Using  $\log r$  against  $T$  plots we have separated the ionic ( $\sigma_i$ ) and electronic ( $\sigma_e$ ) parts of conductivity. Their variation with temperature is shown in Figs 1, 2 and 3 for  $\text{Li}_2\text{MoO}_4$ ,  $\text{Li}_2\text{WO}_4$  and  $\text{Li}_2\text{SO}_4$  as  $\log \sigma_i T$  and  $\log \sigma_e T$  against  $T^{-1}$  plots. Because theories of ionic and electronic transport are quite different, it is more appropriate to present the analysis of these plots separately.

### 3.1. Ionic conductivity

The plots of  $\log \sigma_i T$  against  $T^{-1}$  for the solids studied are given in the appropriate figures. It is seen from these figures that almost no difference exists between  $\sigma$  and  $\sigma_i$  values at higher temperatures but they differ slightly at lower temperatures. In general,  $\log \sigma_i T$  plots are linear in some temperature ranges and can be

TABLE III Percentage of ionic ( $\sigma_i$ ) and electronic ( $\sigma_e$ ) contribution to total conductivity ( $\sigma$ ) at different temperatures

$T$ (K)	Percentage contribution in					
	$\text{Li}_2\text{MoO}_4$		$\text{Li}_2\text{WO}_4$		$\text{Li}_2\text{SO}_4$	
	$\sigma_i$	$\sigma_e$	$\sigma_i$	$\sigma_e$	$\sigma_i$	$\sigma_e$
500	90	10	93	07	81	19
600	91	09	93	07	82	18
700	92	08	94	06	83	17
800	92	08	97	03	89	11
900	92	08	99.7	–	96	04
1000	–	–	99.9	–	99.99	–
1100	–	–	–	–	99.99	–

divided into three regions: (i) linear region below certain temperature  $T_1$ , (ii) non-linear region for temperature  $T_1 < T < T_2$ , (iii) flat and linear region for  $T > T_2$ . Temperatures  $T_1$ ,  $T_2$  and  $T_3$  are different for all three solids. The third region has not been observed for  $\text{Li}_2\text{MoO}_4$ . In these linear ranges the variations of  $\sigma$  and  $S$  can be represented by the equations

$$T\sigma_i = C \exp(-E_a/kT) \quad (4)$$

and

$$S = \frac{\eta}{eT} + H \quad (5)$$

where  $C$  is the temperature-independent constant and  $E_a$  is the activation energy,  $\eta$  is the slope of the  $S$ - $T^{-1}$  plot and  $H$  is a constant. The values of all these parameters are given in Table IV.

In the third temperature region, which has not been observed for  $\text{Li}_2\text{MoO}_4$ ,  $\sigma_i$  values are very high ( $\sim 100 \Omega^{-1} \text{m}^{-1}$ ) and activation energy is not large (Table IV). Thus this is the superionic phase region of these solids. Our data in this region resemble quite well with those of Kvist and Lunden [3] for  $\text{Li}_2\text{WO}_4$ . However, in the case of  $\text{Li}_2\text{SO}_4$  there exists some discrepancy. Kvist and Lunden [3] observed that the  $\sigma$  value of this salt jumps at 846 K and reaches a value of the order of  $100 \Omega^{-1} \text{m}^{-1}$ . We have found that at 847 K there is a small jump in  $\sigma$ , but it does not reach the superionic range. Instead,  $\sigma$  values increase with

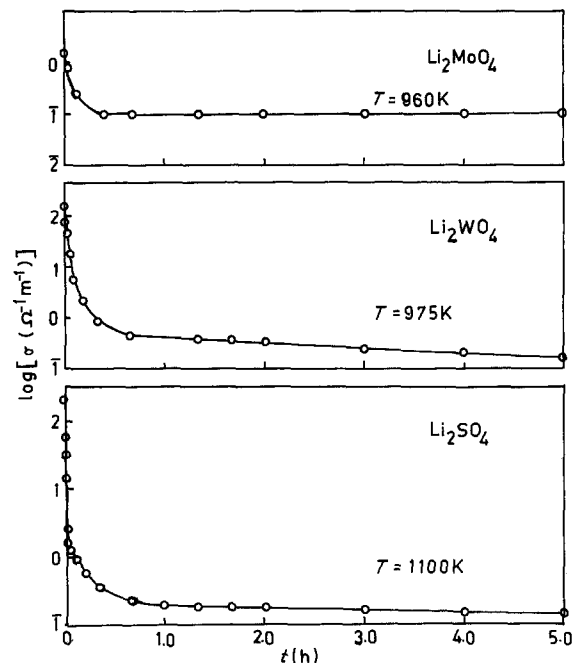


Figure 4 Plots of  $\log \sigma$  against time ( $t$ ) for the studied compounds.

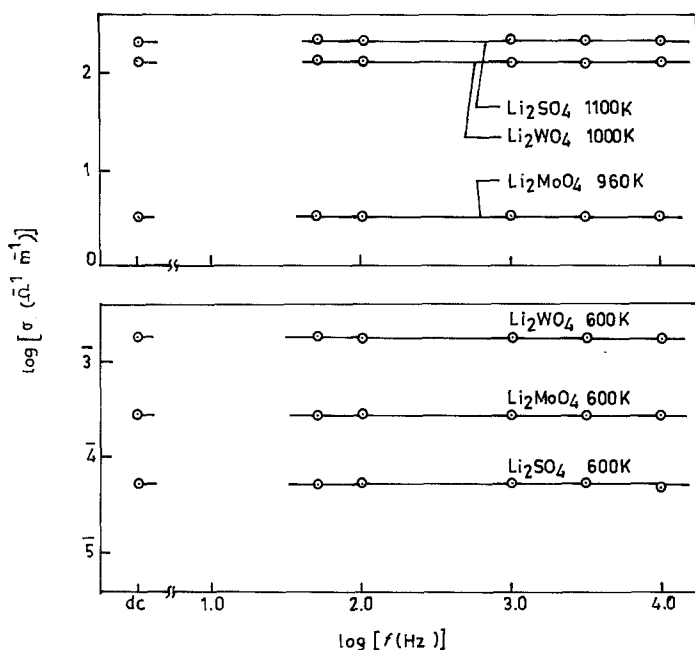


Figure 5 Plots of  $\log \sigma$  against  $\log f$  for the studied compounds, where  $f$  = frequency.

TABLE IV Summarized results of electrical conductivity and thermoelectric power of the compounds studied

Compound	$\sigma$						$S$							
	$T < T_1$		$T > T_2$				$T < T_1$			$T > T_2$				
	$E_a$ (eV)	$C$ ( $\Omega^{-1} \text{m}^{-1}$ )	$T_1$ (K)	$T_2$ (K)	$E_a$ (K)	$C$ ( $\Omega^{-1} \text{m}^{-1}$ )	$\eta$ (eV)	$H$ ( $\text{mV K}^{-1}$ )	Sign	$T_1$ (K)	$T_2$ (K)	$\eta$ (eV)	$H$ ( $\text{mV K}^{-1}$ )	Sign
$\text{Li}_2\text{MoO}_4$	0.67	$7.12 \times 10^4$	700	-	-	-	0.21	0.01	+	830	-	-	-	-
$\text{Li}_2\text{WO}_4$	0.85	$4.00 \times 10^6$	910	960	0.25	$2.89 \times 10^5$	0.67	0.01	+	540	910	-0.33	0.23	-
$\text{Li}_2\text{SO}_4$	1.12	$2.11 \times 10^8$	840	1000	0.41	$1.85 \times 10^7$	0.72	0.36	+	670	1000	-0.64	0.16	-

temperature and reach a value of  $171 \Omega^{-1} \text{m}^{-1}$  at 1000 K. Above 1000 K there is a bending of the  $\log \sigma_i T^{-1}$  plot. Thus the real superionic phase of this material which can be utilized for application purposes in 1000 to 1133 K. The electronic conductivity in this range is negligibly small and hence both  $\sigma$  and  $S$  should arise entirely due to ions. Thus the slope of the  $S-T^{-1}$  plot in this region gives the heat of transport ( $Q$ ) for the mobile ion and the slope of the  $\log \sigma T^{-1}$  plot, its activation enthalpy ( $h_m$ ). The same is true for  $\text{Li}_2\text{WO}_4$ . It is seen from Table IV that  $\eta (=Q) > E_a (=h_m)$  in this range, which is a result not predicted by the common models of superionic solids [21–23]. In fact the mechanism of electrical conduction is well established in  $\text{Li}_2\text{SO}_4$  [24, 25] and is quite different. It belongs to a rotator group of solid electrolyte where not only a large number of equal energy sites are available for  $\text{Li}^+$  ions compared to their number, but also rotation disorder of the  $\text{SO}_4$  group helps in enhancing the  $\text{Li}^+$  ion conductivity. The similarity of the data indicates that the same mechanism is true for  $\text{Li}_2\text{WO}_4$ .

In the lower temperature range, which is the normal phase, there is appreciable ( $\sim 10\%$  to  $20\%$ ) electronic

contribution to  $\sigma$ . The sign of  $S$  in this temperature range is positive which indicates that current carriers are negatively charged. This can happen only when either cation vacancies or anions are mobile. The mobility of anions and thus the occurrence of intrinsic ionic conduction does not seem probable at such a low temperature. Hence conduction in this temperature range seems to be dominated by cation vacancies or Schottky-type defects.

TABLE V Summarized results of electronic contribution to electrical conductivity of the solids studied (general expression  $\sigma_e T = \sigma_0 (-W/kT)$ )

Compound	$W$ (eV)	$\sigma_0$ ( $\Omega^{-1} \text{m}^{-1} \text{K}$ )	$T_p$ (K)
$\text{Li}_2\text{MoO}_4$	0.63	$3.31 \times 10^3$	-
$\text{Li}_2\text{WO}_4$	0.74	$1.08 \times 10^5$	$957 \pm 5$
$\text{Li}_2\text{SO}_4$	1.25	$3.20 \times 10^6$	$847 \pm 5$

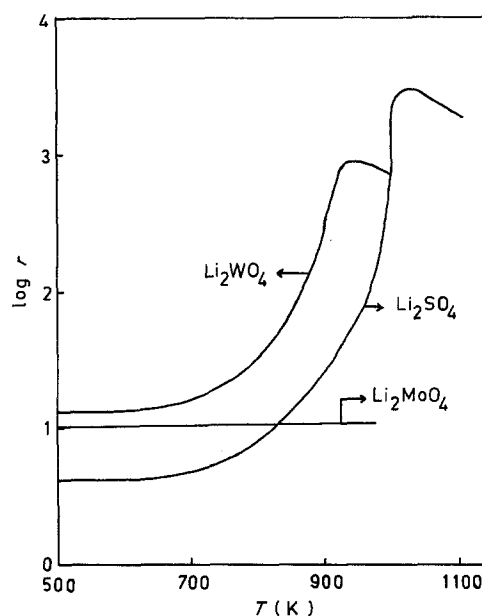


Figure 6 Plots of logarithm of the ratio of ionic and electronic conductivities ( $\log r$ ) against absolute temperature ( $T$ ) for the compounds studied.

In the non-linear region,  $\sigma$  jumps around a particular temperature which we call the transition temperature ( $T_p$ ). The evaluated values of this temperature are  $957 \pm 5$  K for  $\text{Li}_2\text{WO}_4$  and  $847 \pm 5$  K for  $\text{Li}_2\text{SO}_4$ .

### 3.2. Electronic conductivity

The  $\log \sigma_e T - T^{-1}$  plots (Figs 1 to 3) are similar to  $\log \sigma T - T^{-1}$  plots for these materials. The electronic conductivity jumps by several orders of magnitude at the same temperature at which one observes a jump in  $\sigma$ . We have termed this the phase transition temperature. Thus it appears that at the phase transition temperature there occurs a structural change in these solids. Below this temperature the  $\log \sigma_e T - T^{-1}$  plot is linear and can be represented by the equation

$$\sigma_e T = \sigma_0 \exp(-W/kT) \quad (6)$$

where  $\sigma_0$  is a constant and  $W$  is the activation energy for electronic conduction. Values of  $\sigma_0$ ,  $W$  together with the phase transition temperature are given in Table V.

It is seen from this table that the value of  $W$  is large but not large enough to relate it to the energy band gap of the solid. It seems that electronic conduction occurs due to hopping of electrons trapped at defect centres.

### Acknowledgements

K.G. and A.J.P. thank CSIR and UGC, respectively, for financial assistance.

### References

1. A. BENRATH and K. DREKOPF, *Z. Phys. Chem.* **99** (1921) 55.
2. A. KVIST and A. LUNDEN, *Z. Naturforsch.* **20a** (1965) 235.
3. *Idem, ibid.* **21a** (1966) 1509.
4. I. D. RAISTRICK, C. HO and R. A. HUGINS, *Mater. Res. Bull.* **11** (1976) 953.
5. J. B. BOYCE and J. C. MIKKELSEN Jr, *Solid State Commun.* **31** (1979) 741.
6. R. T. JONSON Jr, R. M. BIEFELD and J. D. KECK, *Mater. Res. Bull.* **12** (1977) 577.
7. R. J. JONSON Jr and R. M. BIEFELD, in "Fast Ion Transport in Solids", edited by P. Vashishta, J. Mundy and G. K. Shanoy (North Holland, Amsterdam, 1979) p. 457.
8. K. SINGH and V. K. DESHPANDE, *Solid State Ionics* **13** (1984) 157.
9. K. SHAHI, H. B. LAL and S. CHANDRA, *Ind. J. Pure Appl. Phys.* **13** (1975) 1.
10. O. P. SRIVASTAVA, PhD thesis, University of Gorakhpur (1983).
11. C. TNBUNDT, *J. Electrochem. Soc.* **26** (1920) 358.
12. *Idem*, in "Handbuch der Experimental Physik", **Band XII 1** Teil (1932) p. 383.
13. C. C. LIANG and L. H. BARNETTE, *J. Electrochem. Soc.* **123** (1976) 453.
14. B. K. VERMA and H. B. LAL, *Mater. Res. Bull.* **16** (1981) 1579.
15. J. B. GOODENOUGH, personal communication.
16. A. J. PATHAK, K. GAUR and H. B. LAL, *J. Mater. Sci. Lett.* **5** (1986) 785.
17. *Idem, ibid.* **5** (1986) 1058.
18. A. LUNDEN, A. BENGZELIUM, R. KABER, L. NILSSON, K. SCHROERDER and TARNEBERG, *Solid State Ionics* **9-10** (1983) 89.
19. C. D. HODGEMAN, R. C. WEST and S. M. SELVY, in "Hand Book of Physics and Chemistry" (Chemical Rubber Co., Cleveland, Ohio, 1958) p. 548.
20. A. J. NORD, *Chem. Commun. Univ. Stockholm* **3** (1973) (see also "International Tables for X-ray Crystallography" (Kynoch, Birmingham, 1974).
21. M. J. RICE and W. L. ROTH, *J. Solid State Chem.* **4** (1972) 294.
22. C. P. FLYNN, in "Point Defects and Diffusion" (Oxford University Press, 1972).
23. W. J. PARDEE and G. D. MAHAN, *J. Solid State Chem.* **15** (1975) 310.
24. G. D. MAHAN, *Phys. Rev.* **B14** (1976) 780.
25. R. ARONSSON, H. B. GUNILLAKNAPE, A. LUNDEN, L. NILSSON, L. M. TORELL, N. H. ANDERSEN and J. K. KJEMS, *Rad. Effects* **75** (1983) 79.

Received 12 April  
and accepted 7 September 1988